Oxygen content of YBaCuO thin films

S. Degoy [a], J. Jiménez [b,*], P. Martin [b], O. Martinez [b], A.C. Prieto [c],
D. Chambonnet [a], C. Audry [a], C. Belouet [a], J. Perrière [d]

[a] *Alcatel Alsthom Recherche, Route de Nozay, 91460 Marcoussis, France*
[b] *Fisica de la Materia Condensada, ETS Ingenieros Industriales, 47011 Valladolid, Spain*
[c] *Cristalografia y Mineralogia, Facultad de Ciencias, 47011 Valladolid, Spain*
[d] *Groupe de Physique des Solides, Université Paris 7, 75005 Paris, France*

Received 14 August 1995; revised manuscript received 20 October 1995

Abstract

YBCO thin films are studied by means of Raman spectroscopy and X-ray diffraction. Data concerning oxygenation present significant dispersion as obtained from one or the other technique. This reveals structural distortion in addition to that induced by oxygen vacancies in the Cu–O chains. A linear relation between the frequency of the Raman mode associated with the stretching along the c-axis of the apical oxygen and the deviation of the perfect Ba and Cu stoichiometry is observed. A similar linear relation is obtained as well for the intensity ratio of the high index reflections of the XRD spectrum (I_{006}/I_{005}). Such a relation is not seen for the c-axis length, which suggests that the structural distortion associated with departures from cation stoichiometry is different for $c^*z[Cu(2)]$ and $c^*(1\text{-}2z[Cu(2)])$ in the orthorhombic structure of YBCO. Other factors contributing to the uncertainty in the oxygen assessment in thin films are discussed.

1. Introduction

The availability of high-T_c superconducting thin films has propitiated the use of these materials for the fabrication of high-frequency passive devices, such as resonators, delay lines, filters, antennae [1–3]. One of the main requirements for such applications is the uniformity of the films over relatively large areas, the lack of uniformity being detrimental to the transport properties in the microwave domain [4]. The crystallographic properties of the films are different from those of single crystals. These differences are inherent to the preparation conditions and

concern the stoichiometry, both cations and oxygen, lattice disorder and residual strain. All these factors can induce changes in the structural parameters, making difficult the interpretation of the data obtained from structural analyses, and in particular Raman spectroscopy and X-ray diffraction. Furthermore, such changes can be locally heterogeneous, thus resulting in poor structural homogeneity. Among these parameters, one of the keys for the superconducting properties is the oxygen content, the precise titration of which is of high interest for optimizing the growth processes. The characterization of $YBa_2Cu_3O_{7-x}$ single crystals using Raman spectroscopy has been performed in the last years [5–11], and a reliable relation between Raman observations and the oxygen content has been achieved. Such a

---

* Corresponding author.

systematic study has not been carried out in thin films, for which an extrapolation of the results obtained on single crystals is used. Since the above mentioned growth factors should affect the structural parameters, some disturbance of the Raman spectra may be expected, which may result in discrepancies with the results extrapolated from single-crystal data. A study of the oxygenation of several YBCO thin films grown by the PLD technique, based on the comparison of X-ray diffraction and Raman spectroscopy data is presented in this work. The limitations of the direct application of the results obtained for single crystals to the case of thin films are emphasized.

2. Experimental and samples

Micro-Raman measurements were performed with a DILOR XY Raman spectrometer with multichannel detection. The illumination with an Ar^+ laser was carried out through the objective of an optical microscope. The scattered light was collected by the microscope objective thus conforming a nearly backscattering geometry. The laser power was low enough (≤ 2.5 mW) to prevent sample heating. All the measurements were carried out at room temperature.

YBCO thin films were grown by the PLD (pulsed laser assisted deposition) process. During the deposition, the substrate temperature was set in the 750 to 780°C range and the oxygen pressure in the chamber was 0.2 mbar. The complete procedure has been described elsewhere [12,13]. The growth temperature is indicated in Table 1 for each sample. The substrate was generally (100) MgO, though some films were grown on $SrTiO_3$ buffer layers. The films obtained are highly textured, with their c-axis mostly perpendicular to the substrate surface. X-ray diffraction (XRD) measurements in Bragg–Brentano geometry were carried out in order to determine the c-axis length and the orientation of the films and to calculate the ratio between the intensities of the (006) and (005) reflection lines. The cationic composition of the films was assessed using the RBS (Rutherford backscattering spectroscopy) technique. This technique consists of the backscattering of light ions, either H^+ or $^4He^+$ (in our case $^4He^+$ at 2 MeV), by the heavy cations of the sample. The spectrum of the backscattered ions should depend on the atomic masses, M, and the atomic number, Z, of the atoms forming the studied compound. The energy lost by the scattered ions should depend on the atomic mass, while the number of counts (number of backscattered ions with a given energy) depends on the atomic number through the scattering cross-section. Thus, each cation can be identified by a peak in the ion-backscattered spectrum. The intensity ratio of the different peaks should provide the relative cation composition. A calibration value is needed, in our measurements the results were normalized to an Y content of 1.00 [14].

Table 1
List of samples used for measurements. Substrate, growth temperature, c-axis length, oxygen content determined by Raman, c-axis length and $I(006)/I(005)$ (see text) and deviation from perfect cation stoichiometry $(3.0-[Cu])/3.0)$

Sample	Substrate	$T_{Substr.}$ (°C)	c-axis (nm)	[O] (Raman)	[O] (c length)	[O] (006/005)	$(3.0-[Cu])/3.0$
17762	$SrTiO_3$ (50 nm)/MgO	780	1.1683	6.89	7.00	7.00	
17862	MgO	750	1.1708	6.85	6.83	6.82	
19061	MgO	750	1.1707	6.95	6.84	6.82	
18860-4	MgO	765–780	1.1715	6.92	6.78	6.92	
18863	MgO	765	1.1707	6.87	6.88	6.82	
18863R	MgO	765	1.1718	6.93	6.76	6.74	
2061 *	MgO	750	1.1692	> 7.00	6.93	–	0.050
20760 *	MgO	–	1.1690	> 7.00	6.94	7.00	0.100
219 *	MgO	–	1.1695	6.92	6.91	6.93	0.047
258 *	MgO	765	1.1692	> 7.00	6.93	6.91	0.040
261 *	MgO	760	1.1753	> 7.00	6.54	6.98	0.090

3. Results and discussion

The first-order Raman spectrum of orthorhombic $YBa_2Cu_3O_{7-x}$ presents five A_g Raman active modes, which have been associated with different vibrational modes in the orthorhombic structure of $YBa_2Cu_3O_{7-x}$ [15], namely: stretching of the apical oxygen (O(4)) along the c-axis, labeled O(4) A_g mode (~ 500 cm^{-1}); in-phase c-axis vibration of the O(2)–O(3) oxygen atoms in the CuO_2 planes, labeled O(2,3) A_g mode (~ 440 cm^{-1}); out-of-phase c-axis vibration of the O(2)–O(3) oxygen atoms in the CuO_2 planes, labeled O(2,3) B_{1g} mode (~ 336 cm^{-1}); vertical motion along the c-axis of Cu(2) atoms, Cu(2) A_g mode (~ 145 cm^{-1}); vertical motion along the c-axis of Ba atoms, Ba A_g mode (~ 116 cm^{-1}). A typical Raman spectrum obtained in our films is shown in Fig. 1.

The frequency of the O(4) A_g Raman mode and the c-axis length have been experimentally shown to be sensitive to the oxygen content of $YB_2Cu_3O_{7-x}$ crystals. The frequency of the O(4) A_g Raman mode and the oxygenation have been related through the following empirical relationship [8]:

$$x = 0.027\nu_A - 6.58,$$

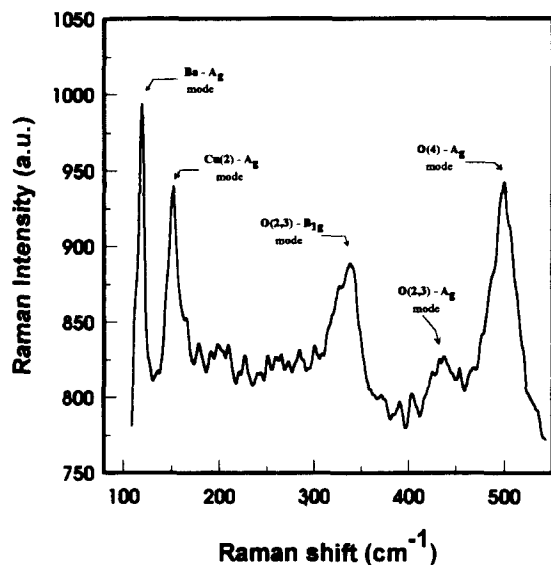where ν_A is the wavenumber of the O(4) A_g mode given in cm^{-1}. On the other hand, oxygenation can

Fig. 1. Typical Raman spectrum of a film showing the five Raman modes (sample 18863).

be calculated from the c-axis length using the following relationship [16,17]:

$$x = (12.771 - c)/0.1557.$$

These formulae provide an accurate estimation of the oxygen content in $YB_2Cu_3O_{7-x}$ crystals, for which they have been sufficiently contrasted. In the case of thin films, these relations need to be handled with care since other factors, as mentioned above, can change the frequency of the O(4) A_g Raman mode, as well as the XRD data.

In this frame, the oxygenation obtained from the c-axis length data was found to be generally inconsistent with the data obtained by Raman spectroscopy for the samples studied in this work. It has also been shown that the c-axis length presented some ambiguities in relation to the oxygenation assessment in thin films [18]. For this reason, it was argued that the intensity ratio of the (006) and (005) reflection lines of X-ray diffraction spectra was more reliable than the c-axis length measurement for oxygen content assessment, when strains occurred in the films in the absence of cation disorder.

Upon this basis, the oxygenation deduced from each one of these analyses was studied for the different samples of Table 1. In view of this data dispersion two different types of samples were considered in Table 1 for a detailed study: samples with different cationic composition and samples grown on different substrates in order to investigate some of the factors that can affect the film properties. The oxygen content, deduced by Raman spectroscopy and XRD, from either the c-axis length or the I_{006}/I_{005} intensity ratio, is given in Table 1. The estimation of the oxygen content using 005 and 006 reflection lines of the XRD spectrum was done using the procedure reported by Ye et al. [18,19] for a series of $YBa_2Cu_3O_{7-x}$ specimens with variable x. A significant data dispersion between these estimations is observed, which suggests that the assessment of the oxygen content in thin films based on structural measurements is by no means ambiguous. These results indicate the existence of different factors affecting in different ways the frequency of the O(4) A_g Raman mode, the length of the c-axis and the intensity ratio of the X-ray reflection peaks. The choice of the 005 and 006 reflection lines was based on the accuracy of the measurement for high index

reflection lines. Some of the films in Table 1 were selected in order to investigate the different factors that may affect the structure of thin films, and in turn, the estimation of the oxygen content. Samples with a poor cationic stoichiometry (with (*) in Table 1) and a sample grown on a 50 nm thick $SrTiO_3$ buffer layer were considered separately.

Samples with poor cationic stoichiometry, after RBS measurement, were selected in order to evaluate the influence of this factor on the Raman spectrum and on the XRD data. In general, these samples are characterized by an anomalously high frequency of the O(4) A_g Raman mode. This high frequency cannot be directly associated with oxygenation, since it would correspond to an oxygen stoichiometry above 7, extrapolating from the empirical relationship between oxygenation and Raman frequency of the O(4) A_g Raman mode. Thus, the high frequency of this Raman mode does not necessarily correspond to a complete oxygenation; but such a frequency shift of the Raman band suggests the existence of structural distortion effects independent of the oxygen content. The observation of such a high frequency seems to be unique for the thin films with incomplete cation stoichiometry; nevertheless in a recent report a similar effect has been observed for crystals obtained by pulling techniques [20].

A comparison of the cationic composition of these samples shows that the larger the deviation from the perfect cationic stoichiometry (either (2.0-[Ba])/2.0 or (3.0-[Cu])/3.0), the larger the blue frequency shift of the O(4) A_g Raman mode, see Fig. 2, where a linear relation between the Raman frequency and the deviation from perfect stoichiometry can be observed. Indeed, samples 20760 and 261 present a strong frequency shift of the O(4) A_g Raman mode, which is correlated with the low Ba and Cu contents of these samples (it should be noted that in all the samples the Cu/Ba ratio remains close to 1.50, thereby the definition of the deviation of the perfect cation stoichimetry as (3.0-[Cu])/3.0)). Since the frequency of the O(4) A_g Raman mode is related to the bond length, $c^* z[Cu(2)]$, of the bridging oxygen, O(4) in the classical notation by Jorgensen [16], a blue frequency shift might be associated with a shorter bond length. In this context, it is interesting to observe that such a behavior is not seen in the relationship between the deviation from cationic stoi-
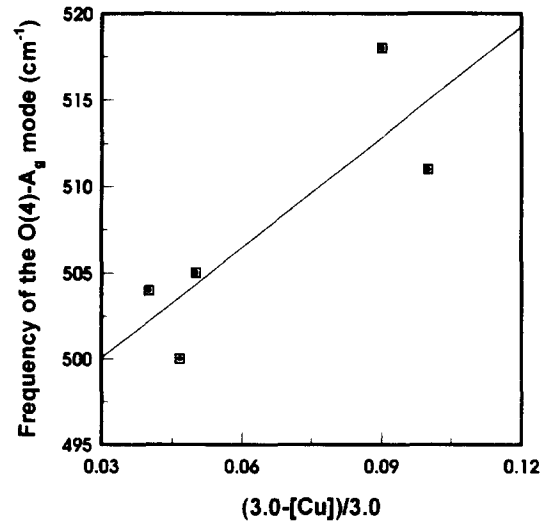

Fig. 2. Frequency of the O(4) A_g Raman mode vs. the deviation of the perfect cation stoichiometry (samples with (*) in Table 1).

chiometry and the c-axis length, see Fig. 3. This would imply that the shortening of the bridging oxygen bond is partially compensated by an increase of the distance between the CuO_2 planes, this being detrimental for the superconducting properties. In fact, one can expect a decrease of the $c^* z[Cu(2)]$ length and a corresponding increase of the $c^*(1 - 2z[Cu(2)])$ length in the structure of orthorhombic
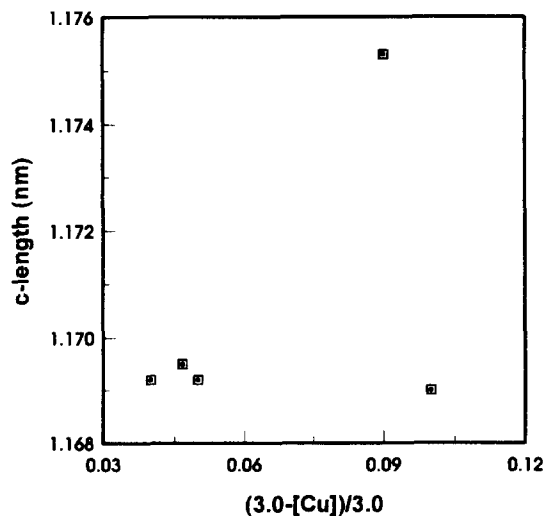

Fig. 3. c-axis length vs. the deviation of the perfect cation stoichiometry (samples with (*) in Table 1).

YBCO. The other Raman modes measured in these samples present a small frequency shift as well, but such a shift is not significant within the experimental accuracy (better than 2 cm^{-1}), which would further support the idea that the bond shortening mainly concerns the bridging oxygen, O(4). Following these ideas, we estimated the $c^* z[Cu(2)]$ length corresponding to the measured Raman frequency, see Fig. 4. The calculation was made extrapolating such a length from the structural data of crystals with variable oxygen content [16]. The distance between CuO_2 planes, $c^*(1 - 2z[Cu(2)])$ was deduced according to the measured c-axis length. Both lengths, $c^* z[Cu(2)]$ and $c^*(1 - 2z[Cu(2)])$, are represented as a function of the deviation from the perfect cation stoichiometry in Fig. 5, exhibiting a linear dependence.

The correlation between the ratio of the integrated intensities of the (005) and (006) reflections and the deviation from the perfect cation stoichiometry is shown in Fig. 6. The relation is significantly similar to that obtained for the frequency of the O(4) A_g Raman mode. The higher dispersion observed in the Raman plot can be understood in terms of the expected higher disorder in the surface of the film,
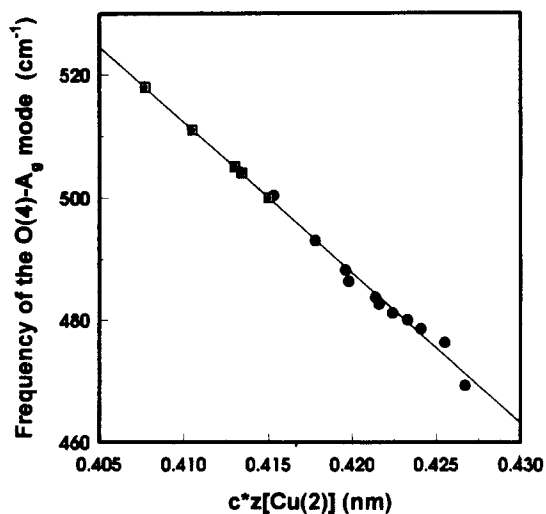

Fig. 5. $c^* z[Cu(2)]$ and $c^*(1 - 2z[Cu(2)])$ lengths as a function of the deviation of the perfect cation stoichiometry.

Fig. 4. Frequency of the O(4) A_g Raman mode vs. the $c^* z[Cu(2)]$ length. The squares are the experimental values measured in films with poor cation stoichiometry (▣). The dark points are the values obtained in $YBa_2Cu_3O_{7-x}$ crystals with variable x. The straight line gives the extrapolated values of $c^* z[Cu(2)]$ for the high Raman frequencies measured in our films.
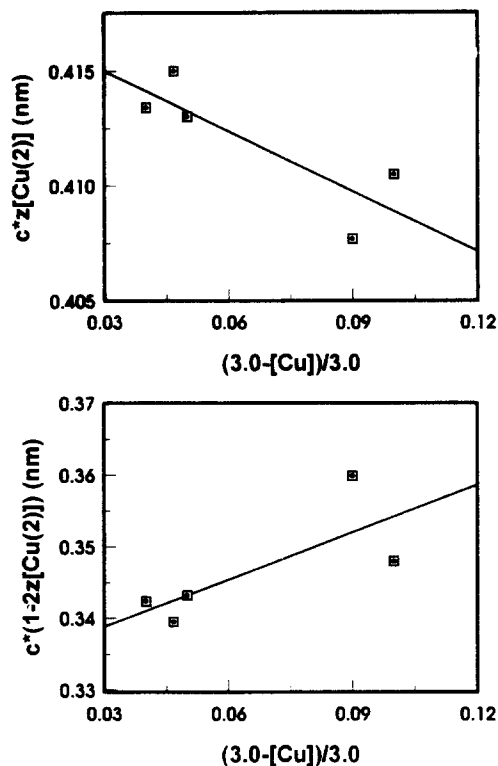
which is the region probed by Raman spectroscopy, as opposed to X-ray diffraction, which probes the film throughout its thickness. It should be noted that all the samples were found to be slightly Ba suppressed at the outer surface, which could also account for the above mentioned dispersion of the Raman data.

Another possible source of disagreement between Raman and X-ray data is the presence of strain in the films. All the samples studied herein were grown on MgO substrates, except sample 17762, which was grown on an MgO substrate coated with a 50 nm thick $SrTiO_3$ buffer layer. This sample was found to have a correct cation stoichiometry. In spite of this, the short c-axis length measured led to an oxygen estimation above 7 and therefore it could be only associated with a full oxygenation. On the other hand, cationic disorder can be ruled out, since it gives an expanded c-axis [19]. Thus, the most reliable hypothesis consists of relating such a short
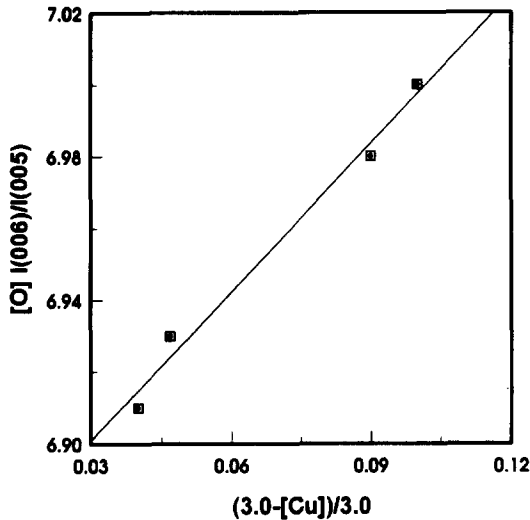
Fig. 6. Oxygen content deduced from I_{006}/I_{005} vs. the deviation of the perfect cation stoichiometry (samples with (*) in Table 1).

c-axis length to compressive stresses along the c-axis. It can arise from in-plane tensile stress, produced by lattice mismatch between the substrate and the film. It should be noted that lattice mismatch for epitaxial films on $SrTiO_3$ is small ($\sim 0.5\%$) [21]; thus, such an effect might arise from a distinct alignment of the grains in the a–b plane, which should result in large-angle grain boundaries, and small grain size. This should strongly depend on the buffer-layer preparation. The influence of the substrate on the film texture has been the object of numerous reports [22,23].

The oxygen content of this sample estimated by Raman spectroscopy was 6.89, which is below the X-ray estimation. It is worth noting that the difference between both experimental methods may arise from the different depth probed by each one: 40 nm for Raman spectroscopy and the complete film thickness, 300–400 nm for XRD. In fact, under compressive stress along the c-axis, the bond length of the apical oxygen should decrease and a blue frequency shift should be observed; since this does not occur, it can be argued that compressive stresses are relaxed in the outer part of the film probed by Raman spectroscopy in contrast to the inner part of the film probed by XRD. To confirm this hypothesis, measurements of the c-axis length against the film thickness will be performed using XRD in grazing inci-

dence. Another possibility should concern the $c_\parallel$ grain orientation probed by Raman spectroscopy according to the A_g symmetry selection rules. This is important, since the stress distribution must be different for grains with the c-axis parallel to the substrate surface, $c_\parallel$, than for grains with the c-axis perpendicular to the substrate surface, $c_\perp$. Since lattice mismatch is different for both orientations [23], tensile strain is expected for $c_\parallel$ grains, against compressive stress for poor epitaxial $c_\perp$ films. Furthermore, oxygen diffusion has been shown to be easier in the a, b directions than in the c direction [24], therefore $c_\parallel$ grains may actually be more oxygenated, which would support again the presence of compressive stress in $c_\perp$ oriented regions. These hypotheses could account for the different oxygen estimates achieved by Raman spectroscopy and c-axis length in specimens with poor $c_\perp$ grain alignment.

As was pointed out before, oxygen assessment by Raman spectroscopy concerns the upper part of the films and the $c_\parallel$ grains due to the Raman backscattering selection rules, while X-rays are probing the whole film, which is mostly $c_\perp$. Nevertheless, the structural factors discussed above are important enough to consider them as the main factors controlling the experimental results presented herein. The assessment of the oxygenation of thin films appears to be a rather complex problem, since the structural transformations associated with the growth conditions of the film strongly influence the Raman and XRD data and make it difficult to separate between the different contributions. Furthermore, it should be noted that cationic stoichiometry, strain, oxygen content and lattice disorder can be spatially distributed, thus contributing to the lack of spatial homogeneity usually found in films.

4. Conclusion

The above results confirm the difficulty to reliably assess the oxygenation of YBCO thin films. It was shown that different factors, arising from the growth conditions, can simultaneously contribute to structural distortions of the orthorhombic lattice of YBCO. These contributions, superimposed to those of the apical oxygen, cannot be isolated in most

cases, thus making difficult the determination of the oxygen content by means of structural analyses, valid for crystals but confusing for thin films. Nevertheless, it has been shown that the c-axis length does not vary with film cationic composition, while Raman spectroscopy and the intensity ratio of (005) and (006) reflection peaks are not sensitive to strains. In the case of Raman spectra this is true for thick films, for which substrate-induced stresses are relaxed in the outer region probed by Raman spectroscopy.

Acknowledgements

References

[1] W. Albrecht, W. Langheinrich, H. Kurz, U. Poppe, H. Stolner and J. Schubert, J. Appl. Phys 68 (1990) 3778.

[2] R. Pinto, P.R. Apte, L.C. Gupta, R. Vijayaraghavan, K. Easwar and B.K. Sarkar, Supercond. Sci. Technol. 4 (1991) 577.

[3] G. Borghs, J. DeBoeck, I. Francois, D. Chambonnet, C. Belouet, Y. Crosnier, J.C. Carru, D. Chauvel, L. Arnaud, H. Boucher, J.C. Villegier, S. Nicoletti, L. Correra and J. Jiménez, J. Phys. IV C 6 (1994) 189.

[4] R. Pinto, N. Goyal, S.P. Pai, P.R. Apte, L.C. Gupta and R. Vijayaraghavan, J. Appl. Phys. 73 (1993) 5105.

[5] C. Thomsen, M. Cardona and R. Liu, J. Less Comm. Met. 150 (1989) 33;
C. Thomsen and M. Cardona, in: High Temperature Semiconductors I and II, ed. D.M. Ginsberg (World Scientific, Singapore, 1989 and 1990).

[6] A. Sacuto and M. Balkanski, J. Alloys Comp. 195 (1993) 359.

[7] G. Burns, F.H. Dacol, C. Feidl and F. Holtzberg, Solid State Commun. 77 (1991) 367.

[8] P.V. Huong, J.C. Bruyère, E. Bustarret and P. Grandchamp, Solid State Commun. 72 (1989) 191.

[9] R. Bhadra, T.V. Brun, M.A. Berro and B. Dabrowski, Phys. Rev. B 37 (1988) 5142.

[10] E. Altendorf, X.K. Chen, J.C. Irwin, R. Liang and W.N. Hardy, Phys. Rev. B 47 (1993) 8140.

[11] K.F. McCarty, J.Z. Lin, R.N. Shelton and H.B. Radonsky; Phys. Rev. B 41 (1990) 8792.

[12] D. Keller, A. Gervais, D. Chambonnet, C. Belouet and C. Audry, J. Phys. III 5 (1995) 135.

[13] D. Chambonnet, C. Belouet, C. Fages and M. Puech, Laser Ablation of Electronic Materials, eds. S. Lazare and E. Fogarassy (North Holland, Amsterdam, 1992) p. 317

[14] For a review see M.A. Nicolet, in: Non-Destructive Evaluation of Semiconductors Materials and Devices, chapter 11, ed. J.N. Zemel (Plenum, New York, 1979).

[15] R. Liu, C. Thomsen, W. Kress, M. Cardona, B. Gegenheimer, F.W. de Wette, J. Prade, A.D. Kulkarni and U. Schoerder, Phys. Rev. B 37 (1988) 7971.

[16] J.D. Jorgensen, B.W. Veal, A.P. Paulikas, L.V. Nowicki, G.W. Crabtree, H. Claus and W.K. Kwok, Phys. Rev. B 41 (1990) 1863.

[17] R.J. Cava, B. Batlogg, C.H. Chen, E.A. Rietman, S.M. Zahurak and D. Werder, Phys. Rev. B 39 (1989) 322.

[18] J. Ye and K. Nakamura, Phys. Rev. B 48 (1993) 7554.

[19] J. Ye and K. Nakamura, Phys. Rev. B 50 (1994) 7099.

[20] O.V. Misochko, S. Tajima, S. Miyamoto, H. Kobayashi, S. Kagiya, N. Watanabe, N. Kozhizuka and S. Tanaka, Phys. Rev. B 51 (1995) 3175.

[21] W.P. Shen, C. Lehane, J.P. Zheng and H.S. Kwok, Appl. Phys. Lett. 64 (1994) 3175.

[22] T. Venkatesan, C.C. Chang, D. Dijkkamps, S.B. Ogale, E.W. Chase, L.A. Farrow, D.M. Hwang, P.F. Miceli, S.A. Schwarz and J.M. Tarascon, J. Appl. Phys. 63 (1988) 4591.

[23] R. Guo, A.S. Bhalla, L.E. Cross and R. Roy, J. Mater. Sci. 9 (1994) 1644.

[24] B.W. Beal, H. You, A.P. Paulikas, H. Shi, Y. Fang and J.W. Downey, Phys. Rev. B 42 (1990) 4770.